Hindawi
International Journal of Polymer Science
Volume 2017, Article ID 3587019, 8 pages
https://doi.org/10.1155/2017/3587019

Research Article

Fabrication and Assessment of ZnO Modified Polyethersulfone Membranes for Fouling Reduction of Bovine Serum Albumin

Tshepo Duncan Dipheko,[1] Kgabo Philemon Matabola,[2] Kate Kotlhao,[3] Richard M. Moutloali,[4] and Michael Klink[3]

[1]*Faculty of Agriculture, Science and Technology, Department of Chemistry, Department of Agriculture, North-West University, Mafikeng Campus, Private Bag X2046, Mmabatho 2735, South Africa*
[2]*Advanced Materials Divisions, DST/Mintek Nanotechnology Innovation Centre, Mintek, Randburg, South Africa*
[3]*Faculty of Applied and Computer Sciences, Department of Chemistry, Vaal University of Technology, Private Bag X021, Vanderbijlpark 1911, South Africa*
[4]*DST/Mintek Nanotechnology Innovation Centre-Water Research Node, University of Johannesburg, P.O. Box 17011, Doornfontein, Johannesburg 2028, South Africa*

Correspondence should be addressed to Kate Kotlhao; katekotlhao@gmail.com and Michael Klink; michaelk1@vut.ac.za

Received 21 October 2016; Accepted 4 December 2016; Published 19 January 2017

Academic Editor: Bernabé L. Rivas

ZnO/PES composite membranes were fabricated by phase inversion method using DMAc as a solvent. The structure of ZnO was investigated using TEM, SEM, XRD, and TGA. TEM images of ZnO nanoparticles were well-defined, small, and spherically shaped with agglomerated nanoparticles particles of 50 nm. The SEM and XRD results were an indication that ZnO nanoparticles were present in the prepared ZnO/PES composites membranes. Contact angle measurements were used to investigate surface structures of the composite membranes. The amount of ZnO nanoparticles on PES membranes was varied to obtain the optimal performance of the composite membranes in terms of pure water flux, flux recovery, and fouling resistance using the protein bovine serum albumin (BSA) as a model organic foulant. The results showed that addition of ZnO to PES membranes improved the hydrophilicity, permeation, and fouling resistance properties of the membranes. Pure water flux increased from a low of 250 L/m^{2}h for the neat membrane to a high of 410 L/m^{2}h for the composite membranes. A high flux recovery of 80–94% was obtained for the composite membranes. The optimal performance of the composite membranes was obtained at 1.5 wt% of ZnO.

1. Introduction

The use of polyethersulfone (PES) in the preparation of membranes for water treatment is widespread [1–4]. This is primarily because the high mechanical strength properties of the polymer material used in fabricating the membranes make its application in water treatment desirable. The main drawback of the membranes produced from PES is that they are relatively hydrophobic and have an inherent problem of fouling [5–8].

Several approaches have been explored to alleviate the fouling problem of PES membranes. These are grafting of the membranes with surface functionalities to enhance hydrophilic surface characteristics [9–11], impacting substances with catalytic properties to degrade foulants on the membrane surface [12–14], and impacting substances with antibacterial effects to limit the adhesion of biomolecules/bacteria that lead to biofouling [4, 15, 16]. Incorporating nanoparticles to increase surface hydrophilicity of the membranes in water treatment has received more attention, recently. This is due to their antibacterial characteristics, high surface to volume ratio, and photocatalytic activity [4, 9, 12, 17].

Titanium dioxide (TiO_2) is among the commonly used nanoparticles for enhancing surface hydrophilicity and water permeation [9, 17, 18]. However, the extensive use of TiO_2

Table 1: Composition of the casting solution used to prepare ZnO/PES membrane composites.

Membranes		PES wt.%	PVP wt.%	ZnO wt.%	DMAc wt.%
Pure PES	A	18	2	0	80
PES/ZnO	B	18	2	0.5	80
PES/ZnO	C	18	2	1	80
PES/ZnO	D	18	2	1.5	80
PES/ZnO	E	18	2	2	80

nanoparticles has over time shown that its photocatalytic activity is limited [19]. Due to this limitation, more research efforts have been directed towards making its application in water treatment effective. Among others is the use of dopants like silver, platinum, and gold as examples [20–22].

On the other hand, ZnO received less attention compared to TiO_2. However, it has similar or better desirable properties such as large surface area to volume ratio, mechanical and chemical properties, and photocatalysis (with a higher band gap than TiO_2). It is more cost-effective than TiO_2 [23]. These properties have widened its application to various areas such as solar cells [24], biosensors [25], and photocatalysis [26–28] and recently in water treatment [29, 30].

The positive improvement of nanoparticles incorporated into membranes in water treatment depends on their ability to enhance surface hydrophilicity and water permeability. When ZnO nanoparticles were incorporated into PES, a low flux decline and better permeability were obtained [23]. Another study by Leo et al. [31] showed a significant reduction on hydrophobicity of the ZnO/polysulfone (Psf) membrane and an improvement on the fouling resistance by oleic acid. Shen et al. [32] used bovine serum albumin (BSA) as a protein foulant on ZnO/PES composite membranes and indicated that there was essentially no change on BSA rejection ratio from the lowest amount (0.1) of ZnO to the highest (0.4). This could mean that addition of ZnO had no effect on pore size of the PES membranes. The other reason could be that the increase in pore size did not exceed the molecular weight of the protein, BSA. These results were in agreement with that observed by Balta et al. [23]. Contrary to the results by Shen et al. and Balta et al., addition of ZnO nanoparticles into polyvinylidene fluoride (PVDF) membrane had some effect on the rejection of the model foulant [33]. Another point to note from Shen et al. paper is that the ZnO/PES membranes were prepared using polyethylene glycol (PEG-400) additive and N-methyl pyrrolidone (NMP) as solvent.

In the present study, the objective was to prepare ZnO embedded PES membranes by phase inversion method using DMAc (as a solvent) and polyvinylpyrrolidone (PVP) (as pore former additive and to reduce aggregation of nanoparticles) to improve water permeation and fouling resistance. It has been indicated that DMAc enhances porosity far much better than NMP and that high porosity leads to high water fluxes [32, 34]. The ZnO/PES membranes' performance was investigated through pure water flux and flux recovery using BSA as model organic foulant. The amount of ZnO nanoparticles for optimal performance of the ZnO/PES composite membranes was investigated.

2. Experimental Section

2.1. Materials and Equipment. Polyethersulfone (PES MW = 232.258 g/mol) was supplied by Solvay Plastics. Dimethylacetamide (DMAc), polyvinylpyrrolidone (PVP MW = 10,000 g/mol), zinc acetate dihydrate ($Zn(CH_3COO)_2 \cdot 2H_2O$), sodium hydroxide (NaOH), and bovine serum albumin (BSA, MW = 66000 Da) were obtained from Sigma-Aldrich. All reagents were used without any further purification. Freshly deionized water was used in all the preparations.

2.2. Synthesis of Zinc Oxide Nanoparticles. ZnO nanoparticles were synthesized using established protocols [28, 35, 36]. In short, aqueous solution of NaOH (0.4 M) was added dropwise into an aqueous solution of zinc acetate ($Zn(CH_3COO)_2 \cdot 2H_2O$, 0.2 M) to induce precipitation of zinc hydroxide nanoparticles at 60°C, pH = 12.0, for 1 h. The mixture was left to stir under these conditions for a further 1 h. The reaction mixture was cooled down to room temperature, centrifuged, and washed with copious amount of water and ethanol for effective removal of impurities. The final product was dried at 60°C for 24 h and subsequently calcined at 500°C overnight.

2.3. Preparation of Membranes. Neat PES membranes were prepared via phase inversion induced by immersion precipitation [11, 37, 38]. A DMAc solution of PES (18 wt.%) and PVP (2 wt.%) was prepared. Following the complete dissolution of the polymers, varying amounts of ZnO nanoparticles (0, 0.5, 1, 1.5, and 2 wt.%) were introduced and the resultant mixture agitated through vigorous stirring until a consistent mixture was obtained, in about 12 h [39]. The polymer-ZnO homogeneous mixture was first degassed under vacuum for 4 h and subsequently spread on a glass plate and cast using an automated knife. The cast film was immersed into an aqueous bath after 30 s in air. The formed membrane that peeled from the glass plate was stored in fresh water for 18 h to allow complete solvent removal from the film. Composition of the reagents used in preparation of ZnO/PES is shown in Table 1.

2.4. Characterisation of ZnO Nanoparticles. The surface morphology of zinc oxide nanoparticles was studied using the transmission electron microscopy (TEM). TEM is a technique used to produce images of a sample by passing a beam of electrons through a sample. TEM is based on transmitted electrons. The beam of electrons interacts with the sample forming images. TEM images are focused onto an imaging

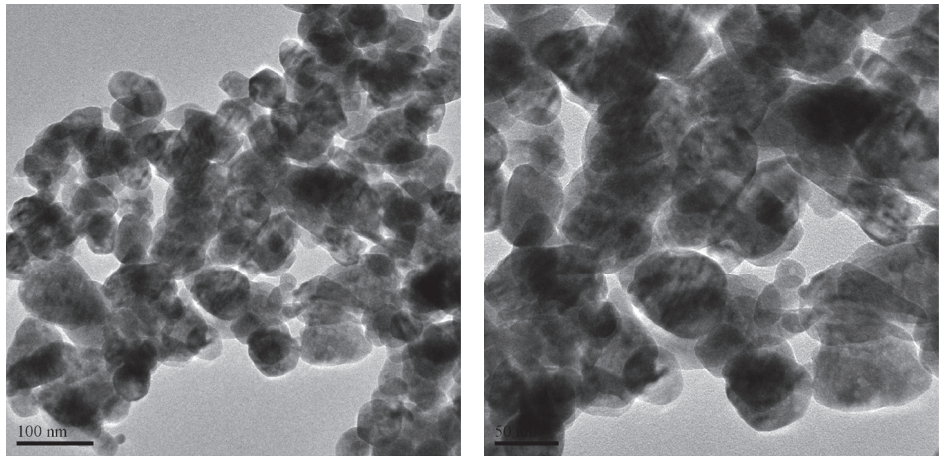

Figure 1: TEM images of ZnO nanoparticles.

device. TEM has a high magnification that can go into the nanoscale range and therefore can be used to see what is inside the material, that is, beyond the surface of the material.

2.5. Characteristics of Membrane Surface. The physical characteristics of the membranes were assessed using a combination of techniques, including scanning electron microscopy (SEM), atomic force microscopy (AFM), contact angle (CA), X-ray diffraction (XRD), and thermal analysis (TA). In order to visualise the membrane surface structure and morphology, membranes were assessed using scanning electron microscope (SEM, FEI NOVA-nanoSEM 200). The samples were coated by sputtering with gold and the micrographs obtained at operating voltage of 30 keV and the current of 10 mA Contact angles of the prepared membranes were measured using a DSA 10 Mk2 (Krüss, Germany) equipment. A water drop was lowered onto the membrane's surface from a needle tip and a magnified image of the droplet was recorded by a digital camera until no further changes were observed. Static contact angles were determined from these images with calculation software. To minimize the experimental error, the contact angle measurement was taken as the mean value of 5 different points on each membrane sample. To confirm the presence of nanoparticles in the membranes, the X-ray diffraction analysis was done using a Bruker equipment (D8 ADVANCE axes) with a monochromatic Cu Kα radiation (λ = 0.154 nm) source operated at 40 mA and 40 kV between 20° and 70°. Finally, thermal analysis of the membranes were evaluated using simultaneous thermal analyser (Netzsch, STA429 CD) under a nitrogen atmosphere at a heating rate of 10°C/min. from 20°C to 800°C.

2.6. Membrane Performance. The performance of the membrane was measured through permeation flux, pure water permeability (membrane hydraulic resistance), and flux recovery after passing protein bovine serum albumin (BSA) as the model foulant. The pure water flux was obtained from a filtration system that contained a Sterlitech HP4750 dead-end stirred filtration cell with an effective area and volume of 14.6 cm^2 and 250 mL, respectively. The nitrogen gas compressed in a cylinder gas was controlled by a regulator. The procedure involved first compacting the membranes at 150 KPa for 30 min, followed by reducing the operating pressure to 100 KPa to obtain the membrane performance at ambient temperature.

Pure water flux (J_{wi}) was obtained after a steady flow was reached and calculated using

$$J_{wi} = \frac{V}{A \cdot t}, \tag{1}$$

where J_{wi} is the pure water flux (L/m^2h), V is the permeate volume (L), A is the membrane area (m^2), and t is the time (h). Average flux was calculated from an average obtained from five samples per membrane cast with five measurements for each sample.

In obtaining the flux recovery (FR), the membranes used for BSA rejection were rinsed with deionized water by filling and shaking the cell for 1 min. three times. Thereafter, the deionized water flux (J_{ww}) was measured again using the cleaned membrane. The flux recovery (FR) was calculated utilising the following equation:

$$\text{FR\%} = \frac{J_{ww}}{J_{wi}} \times 100, \tag{2}$$

where J_{ww} and J_{wi} are the pure water flux of fouled and virgin membranes, respectively.

3. Results and Discussions

3.1. ZnO Nanoparticles Morphology. The morphology of zinc oxide was studied using the TEM. The micrograph was taken at 100 nm as shown in Figure 1.

TEM studies were carried out to find out the structure and exact particle size of the synthesized ZnO. The structure of ZnO nanoparticles mainly adopted a hexagonal configuration. The number of alternating planes composed of tetrahedral coordinated O^{-2} and Zn^{+2} ions is stacked alternatively along c-axis [40]. TEM images of ZnO nanoparticles are well-defined, small, and spherically shaped with agglomerated

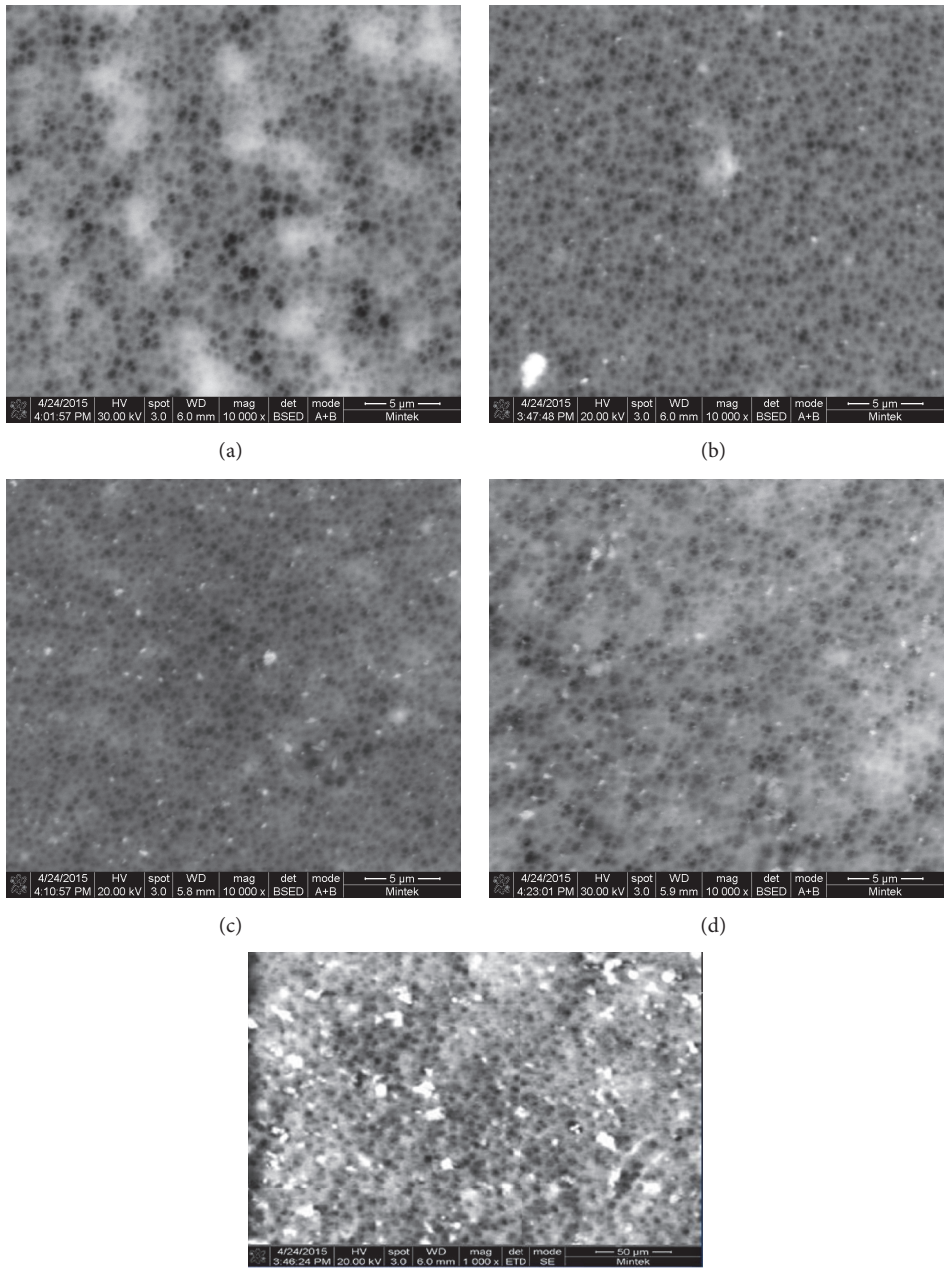

Figure 2: SEM images of (a) pure PES; (b) PES/ZnO (0.5%); (c) PES/ZnO (1.0%); (d) PES/ZnO (1.5%); (e) PES/ZnO (2.0%).

particles. TEM images, in Figure 1, show particle size of ZnO nanoparticles in the range of 50 nm–80 nm.

3.2. Membrane Physical Property Characterisation

3.2.1. SEM Analysis of the Membrane Surfaces. The surfaces of the fabricated membranes were observed using SEM. Figure 2 shows the neat PES membranes as well as those containing ZnO nanoparticles. From the micrographs, the surfaces before and after addition of the nanoparticles remained essentially the same. This was true for all membranes; however, at the highest amount of ZnO nanoparticles (2 wt%) added, clustering of nanoparticles was evident. All the membranes exhibited similar pore-like structure on their surfaces.

3.2.2. Surface Hydrophilicity of the Membranes Using Contact Angle Measurement. The contact angle (CA) is the angle at which the liquid meets the solid surface. The surface can be classified as hydrophobic or hydrophilic, if the CA is $90^\circ < \theta < 180^\circ$ or $0 < \theta < 90^\circ$, respectively [41]. Contact angles (CA) of all membranes were measured at 25°C and the recorded values are an average of five readings. The CA of the membranes showed a steady decline with

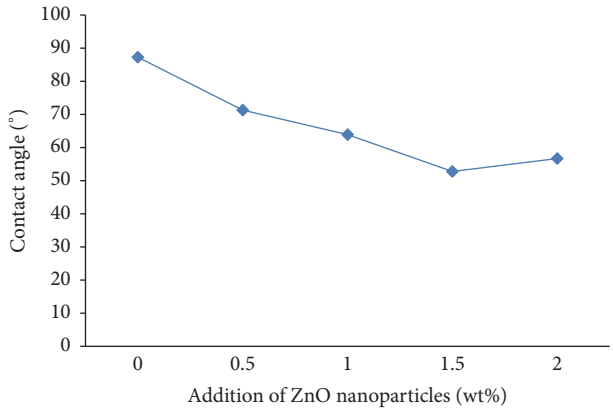

Figure 3: Contact angle measurements of composite ZnO/PES membranes at different amounts of ZnO nanoparticles from (0, 0.5, 1, and 1.5 to 2 wt%).

increasing amount of ZnO nanoparticles (Figure 3). The CA decreased from 87° for the neat membrane to a low of 53° for the composite membrane containing 1.5 wt.% ZnO nanoparticles. This was an indication that ZnO nanoparticles enhanced surface hydrophilicity of the PES membrane. This was attributed to the fact that ZnO has a higher affinity for water [10]. A more hydrophilic membrane surface is expected to improve the water flux and fouling resistance [32].

A sudden increase in CA was observed at 2.0 wt% ZnO. The CA of 64° was recorded at this amount. A similar trend was observed by Damodar et al. (2009) [42] in which the CA of 1 wt% of TiO_2 in TiO_2/PVDF composite membrane was lower than at 4 wt% TiO_2. The apparent reversal of the trend at 2 wt.% of ZnO nanoparticle was attributed to agglomeration and aggregation of nanoparticles on the membrane matrix leading to surface inhomogeneity [42].

3.2.3. XRD Analysis of the Membrane Surfaces. The presence of ZnO nanoparticles in the membrane matrix was confirmed by XRD analysis. Figure 4 shows the diffractograms of unsupported ZnO nanoparticles (A), neat PES (B) membrane, and ZnO containing PES membrane (C). The unsupported ZnO nanoparticles exhibited dominant peaks at 2θ angles of 36.91°, 39.98°, 42.17°, and 55.78° which correspond to the main characteristic peaks of zinc oxide nanoparticles [43, 44]. The neat PES membrane in contrast showed a diffractogram with diffuse broad peaks, indicative of amorphous materials [45]. The composite membrane on the other hand showed characteristic peaks of both the ZnO nanoparticles and neat membrane as expected for such a composite. For example, the ZnO/PES composite membrane had peaks at 2θ angles at 35.62°, 37.73°, 30.20°, and 53.25° which correspond to the unsupported ZnO nanoparticles. The XRD results were an indication that ZnO nanoparticles were present in the prepared ZnO/PES composites membranes [32]. It is worth noting that these diffraction peaks were slightly shifted to lower angles, which was unexpected. Previous studies of ZnO incorporated in PES membrane matrix did not report on the XRD studies. However, similar observations were reported for PES membranes incorporated with TiO_2 nanoparticles [18].

3.2.4. Thermal Analysis of the Membranes. Thermal analysis (TGA) provides information on the decomposition temperature (Td) of a substance. It is defined as the temperature at 3% weight loss [46]. A simultaneous thermal analyser (Netzsch, STA429 CD) was used to investigate the weight loss of both the neat PES and composite membranes. The decomposition temperature of the pure PES and ZnO/PES membrane followed a similar trend. The temperature gradually increased with increasing addition of ZnO on PES membranes (Figure 5). Similar observations were reported by Li et al. (2008) and Wu et al. (2008) [1, 46], when TiO_2 nanoparticles were incorporated into PES membranes. Addition of TiO_2 nanoparticles improved the thermal stability of the PES membranes.

3.3. Effect of ZnO on PES Membrane Performance

3.3.1. Pure Water Flux and Flux Recovery. The dead-end cell was used to measure the filtration properties of the membranes at 25°C. It was observed that the pure water flux of the composite membranes was higher than that of the neat membrane (Figure 6). As the weight of ZnO nanoparticles increased from 0 to 2 wt.%, the water flux of the membrane increased to a peak value and decreased slightly beyond 1.5 wt% ZnO. It increased from a low of 250 L/m^{2}h for the neat membrane to a high of 410 L/m^{2}h for the composite membrane with 1.5 wt.% ZnO. The increasing flux was attributed to increasing permeability of the composite membranes due to incorporation of ZnO nanoparticles [32]. The highest flux was obtained at 1.5 wt.% ZnO nanoparticles in the PES membrane. This corresponds to the lowest contact angle recorded at 1.5 wt.% ZnO nanoparticles (Figure 3). Both the lowest contact angle and the highest flux results were attributed to an enhanced surface hydrophilicity or pore size enlargement [31]. However, pore size determination was not done in this study. At the 2.0 wt% ZnO, there was a reversal which was attributed to pore size and nanoparticle aggregation that lead to pore blockages and hence reduced flux [47].

Figure 6 also shows that flux recovery was influenced by the incorporation of ZnO nanoparticles. Whereas this was at 60% for the neat PES membrane, the composite membranes were between a good recovery of 80 and 94%. The improved flux recovery confirmed that the prepared ZnO/PES composite membranes exhibited enhanced fouling resistance properties.

4. Conclusions

ZnO/PES composite membranes of different amounts of ZnO nanoparticles (0, 0.5, 1.0, 1.5, and 2.0 wt%) were prepared by phase inversion using DMAc as the solvent. TEM images of ZnO nanoparticles were well-defined, small, and spherically shaped with agglomerated nanoparticles particles of 50 nm. The SEM and XRD results were an indication that ZnO nanoparticles were present in the prepared ZnO/PES

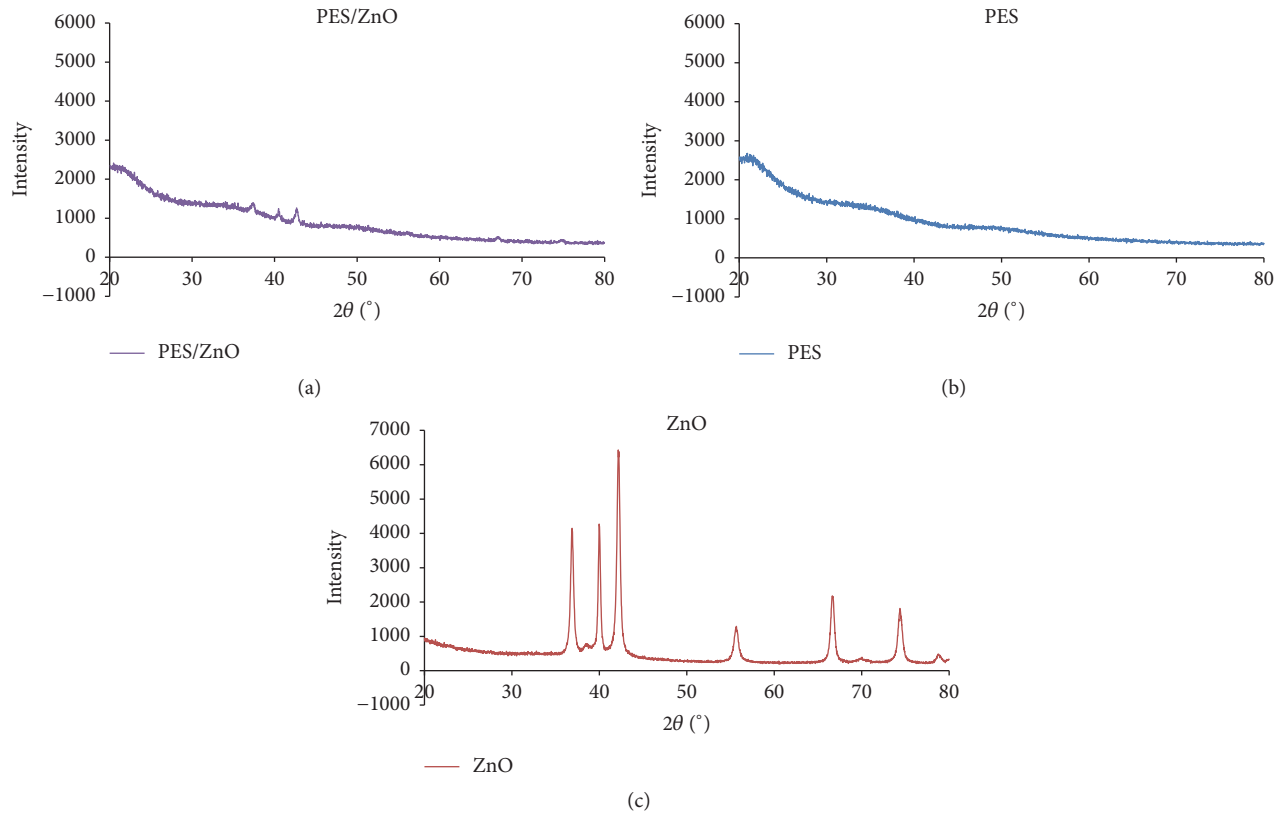

FIGURE 4: XRD patterns of PES membrane: (a) ZnO/PES composite, (b) pure PES, and (c) ZnO nanoparticles.

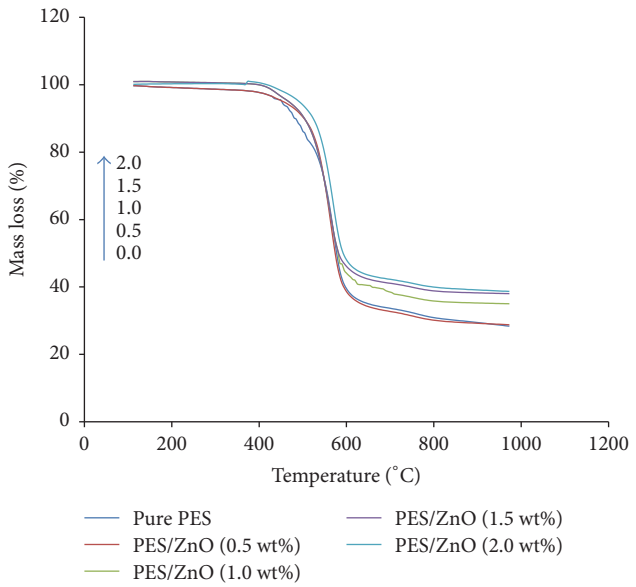

FIGURE 5: TGA results for increasing decomposition temperature for (0.0, 0.5, 1.0, 1.5, and 2.0 wt%) of ZnO on PES membranes.

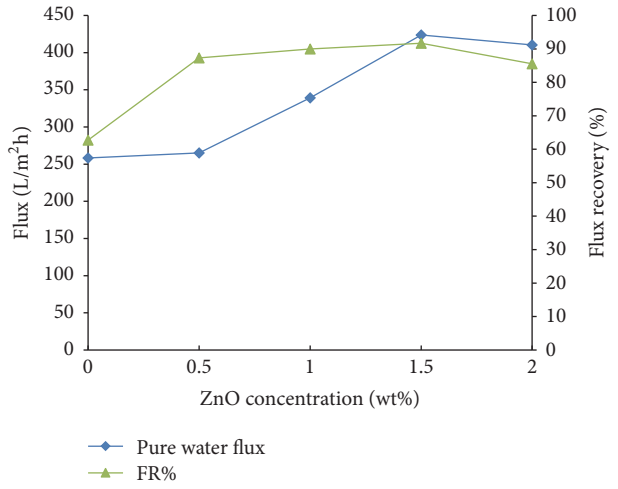

FIGURE 6: Pure water flux and flux recovery, FR% (after filtration of BSA) changes with the addition of ZnO nanoparticles.

composites membranes. Addition of TiO_2 nanoparticles improved the thermal stability of the PES membrane showed by TGA. It was demonstrated that the ZnO/PES composite membranes surface hydrophilicity was greatly improved. The lowest value of ZnO/PES contact angle that corresponded to the highest hydrophilicity was 53°, obtained at 1.5 wt% ZnO nanoparticles. The performance of the membranes showed that pure water flux on ZnO/PES membrane was relatively higher when compared to the neat membrane. Finally, the flux recovery of within 80–94% was obtained for the composite membranes when compared to 60% of the neat

membrane and the optimal performance of the composite membranes was obtained at 1.5 wt% ZnO.

Additional Points

Highlights. (i) Zinc oxide (ZnO) nanoparticles were incorporated into polyethersulfone (PES) membranes. (ii) Addition of ZnO nanoparticles improved the hydrophilicity, permeation, and fouling resistance of the membrane. (iii) The amount of ZnO nanoparticles that produced the optimal hydrophilicity, pure water flux, and flux recovery of the membrane was 1.5 wt%.

Competing Interests

The authors declare that they have no competing interests.

Acknowledgments

The authors appreciate North-West University Chemistry Department, the Advanced Materials Division DST/Mintek, and Vaal University of Technology for providing conducive research platforms to successfully carry out this study. Financial assistance was provided from the National Research Foundation (NRF) and Sasol Inzalo, South Africa.

References

[1] J.-F. Li, Z.-L. Xu, and H. Yang, "Microporous polyethersulfone membranes prepared under the combined precipitation conditions with non-solvent additives," *Polymers for Advanced Technologies*, vol. 19, no. 4, pp. 251–257, 2008.

[2] H. L. Richards, P. G. Baker, and E. Iwuoha, "Metal nanoparticle modified polysulfone membranes for use in wastewater treatment: a critical review," *Journal of Surface Engineered Materials and Advanced Technology*, vol. 2, no. 3, pp. 183–193, 2012.

[3] H. Susanto, N. Stahra, and M. Ulbricht, "High performance polyethersulfone microfiltration membranes having high flux and stable hydrophilic property," *Journal of Membrane Science*, vol. 342, no. 1-2, pp. 153–164, 2009.

[4] K. Zodrow, L. Brunet, S. Mahendra et al., "Polysulfone ultrafiltration membranes impregnated with silver nanoparticles show improved biofouling resistance and virus removal," *Water Research*, vol. 43, no. 3, pp. 715–723, 2009.

[5] M. Cheryan, *Ultrafiltration Handbook United States of America*, Technomic Publishing Company Inc., Lancaster, Pa, USA, 1986.

[6] A. K. Pabby, S. S. H. Rizvi, and A. M. Sastre, *A Handbook of Membrane Separation: Chemical, Pharmaceutical, Food, and Biotechnological Applications*, CRS Tailor and Francis Group, New York, NY, USA, 2009.

[7] C. H. Koo, A. W. Mohammad, F. Suja', and M. Z. Meor Talib, "Use and development of fouling index in predicting membrane fouling," *Separation and Purification Reviews*, vol. 42, no. 4, pp. 296–339, 2013.

[8] P. S. Singh, K. Parashuram, S. Maurya, P. Ray, and A. V. R. Reddy, "Structure-performance-fouling studies of polysulfone microfiltration hollow fibre membranes," *Bulletin of Materials Science*, vol. 35, no. 5, pp. 817–822, 2012.

[9] M.-L. Luo, J.-Q. Zhao, W. Tang, and C.-S. Pu, "Hydrophilic modification of poly(ether sulfone) ultrafiltration membrane surface by self-assembly of TiO_2 nanoparticles," *Applied Surface Science*, vol. 249, no. 1–4, pp. 76–84, 2005.

[10] P. Bai, X. Cao, Y. Zhang, Z. Yin, Q. Wei, and C. Zhao, "Modification of a polyethersulfone matrix by grafting functional groups and the research of biomedical performance," *Journal of Biomaterials Science, Polymer Edition*, vol. 21, no. 12, pp. 1559–1572, 2010.

[11] Y. Mansourpanah, S. S. Madaeni, A. Rahimpour, Z. Kheirollahi, and M. Adeli, "Changing the performance and morphology of polyethersulfone/polyimide blend nanofiltration membranes using trimethylamine," *Desalination*, vol. 256, no. 1–3, pp. 101–107, 2010.

[12] T. Singh, N. Srivastava, and N. Lal Singh, "Application of TiO_2 nanoparticle in photocatalytic degradation of organic pollutants," *Materials Science Forum*, vol. 855, pp. 20–32, 2016.

[13] A. M. Peiró, J. A. Ayllón, J. Peral, and X. Doménech, "TiO_2-photocatalyzed degradation of phenol and ortho-substituted phenolic compounds," *Applied Catalysis B: Environmental*, vol. 30, no. 3-4, pp. 359–373, 2001.

[14] M. K. Seery, R. George, P. Floris, and S. C. Pillai, "Silver doped titanium dioxide nanomaterials for enhanced visible light photocatalysis," *Journal of Photochemistry and Photobiology A: Chemistry*, vol. 189, no. 2-3, pp. 258–263, 2007.

[15] J. Yin, Y. Yang, Z. Hu, and B. Deng, "Attachment of silver nanoparticles (AgNPs) onto thin-film composite (TFC) membranes through covalent bonding to reduce membrane biofouling," *Journal of Membrane Science*, vol. 441, pp. 73–82, 2013.

[16] J. Huang, H. Wang, and K. Zhang, "Modification of PES membrane with Ag–SiO_2: Reduction of biofouling and improvement of filtration performance," *Desalination*, vol. 336, pp. 8–17, 2014.

[17] K. Gupta, R. P. Singh, A. Pandey, and A. Pandey, "Photocatalytic antibacterial performance of TiO_2 and Ag-doped TiO_2 against S. Aureus. P. Aeruginosa and E. Coli," *Beilstein Journal of Nanotechnology*, vol. 4, no. 1, pp. 345–351, 2013.

[18] J.-F. Li, Z.-L. Xu, H. Yang, L.-Y. Yu, and M. Liu, "Effect of TiO_2 nanoparticles on the surface morphology and performance of microporous PES membrane," *Applied Surface Science*, vol. 255, no. 9, pp. 4725–4732, 2009.

[19] H. Dong, G. Zeng, L. Tang et al., "An overview on limitations of TiO_2-based particles for photocatalytic degradation of organic pollutants and the corresponding countermeasures," *Water Research*, vol. 79, pp. 128–146, 2015.

[20] M. Nasr-Esfahani and M. H. Habibi, "Silver doped TiO_2 nanostructure composite photocatalyst film synthesized by sol-gel spin and dip coating technique on glass," *International Journal of Photoenergy*, vol. 2008, Article ID 628713, 11 pages, 2008.

[21] N. Bahadur, K. Jain, A. K. Srivastava et al., "Effect of nominal doping of Ag and Ni on the crystalline structure and photocatalytic properties of mesoporous titania," *Materials Chemistry and Physics*, vol. 124, no. 1, pp. 600–608, 2010.

[22] B. Rajamannan, S. Mugundan, G. Viruthagiri, N. Shanmugam, and P. Praveen, "Properties of Sol-gel derived silver doped titania nanoparticles," *International Journal of Current Research*, vol. 5, no. 10, pp. 2863–2867, 2013.

[23] S. Balta, A. Sotto, P. Luis, L. Benea, B. Van der Bruggen, and J. Kim, "A new outlook on membrane enhancement with nanoparticles: the alternative of ZnO," *Journal of Membrane Science*, vol. 389, pp. 155–161, 2012.

[24] E. Topoglidis, A. E. G. Cass, B. O'Regan, and J. R. Durrant, "Immobilisation and bioelectrochemistry of proteins on nanoporous TiO_2 and ZnO films," *Journal of Electroanalytical Chemistry*, vol. 517, no. 1-2, pp. 20–27, 2001.

[25] B. N. Aini, S. Siddiquee, K. Ampon, K. F. Rodrigues, and S. Suryani, "Development of glucose biosensor based on ZnO nanoparticles film and glucose oxidase-immobilized eggshell membrane," *Sensing and Bio-Sensing Research*, vol. 4, pp. 46–56, 2015.

[26] Z. L. Wang, "Nanostructures of zinc oxide," *Materials Today*, vol. 7, no. 6, pp. 26–33, 2004.

[27] C. Karunakaran, V. Rajeswari, and P. Gomathisankar, "Optical, electrical, photocatalytic, and bactericidal properties of microwave synthesized nanocrystalline Ag-ZnO and ZnO," *Solid State Sciences*, vol. 13, no. 5, pp. 923–928, 2011.

[28] G. Bandekar, N. S. Rajurkar, I. S. Mulla, U. P. Mulik, D. P. Amalnerkar, and P. V. Adhyapak, "Synthesis, characterization and photocatalytic activity of PVP stabilized ZnO and modified ZnO nanostructures," *Applied Nanoscience*, vol. 4, no. 2, pp. 199–208, 2014.

[29] M. Tan, G. Qiu, and Y.-P. Ting, "Effects of ZnO nanoparticles on wastewater treatment and their removal behavior in a membrane bioreactor," *Bioresource Technology*, vol. 185, pp. 125–133, 2015.

[30] N.-Q. Puay, G. Qiu, and Y.-P. Ting, "Effect of Zinc oxide nanoparticles on biological wastewater treatment in a sequencing batch reactor," *Journal of Cleaner Production*, vol. 88, pp. 139–145, 2015.

[31] C. P. Leo, W. P. Cathie Lee, A. L. Ahmad, and A. W. Mohammad, "Polysulfone membranes blended with ZnO nanoparticles for reducing fouling by oleic acid," *Separation and Purification Technology*, vol. 89, pp. 51–56, 2012.

[32] L. Shen, X. Bian, X. Lu et al., "Preparation and characterization of ZnO/polyethersulfone (PES) hybrid membranes," *Desalination*, vol. 293, pp. 21–29, 2012.

[33] J. Hong and Y. He, "Effects of nano sized zinc oxide on the performance of PVDF microfiltration membranes," *Desalination*, vol. 302, pp. 71–79, 2012.

[34] S. S. Madaeni and A. H. Taheri, "Preparation of PES ultrafiltration membrane for treatment of emulsified oily wastewater: effect of solvent and non-solvent on morphology and performance," *Journal of Polymer Engineering*, vol. 29, no. 4, pp. 183–198, 2009.

[35] S. Talam, S. R. Karumuri, and N. Gunnam, "Synthesis, characterization, and spectroscopic properties of ZnO nanoparticles," *ISRN Nanotechnology*, vol. 2012, Article ID 372505, 6 pages, 2012.

[36] Y. S. Patil and I. D. Patil, "Synthesis and charactreization of zinc oxide nanostructures," *International Journal of Science, Spirituality, Business and Technology*, vol. 2, pp. 88–91, 2014.

[37] A. Rahimpour, S. S. Madaeni, and Y. Mansourpanah, "The effect of anionic, non-ionic and cationic surfactants on morphology and performance of polyethersulfone ultrafiltration membranes for milk concentration," *Journal of Membrane Science*, vol. 296, no. 1-2, pp. 110–121, 2007.

[38] A. Rahimpour, S. S. Madaeni, A. Shockravi, and S. Ghorbani, "Preparation and characterization of hydrophile nano-porous polyethersulfone membranes using synthesized poly(sulfoxide-amide) as additive in the casting solution," *Journal of Membrane Science*, vol. 334, no. 1-2, pp. 64–73, 2009.

[39] H.-T. Yeo, S.-T. Lee, and M.-J. Han, "Role of a polymer additive in casting solution in preparation of phase inversion polysulfone membranes," *Journal of Chemical Engineering of Japan*, vol. 33, no. 1, pp. 180–184, 2000.

[40] A. Bradford, "Rapid and sensitive method for the quantitation of microgram quantities of protein utilizing the principle of protein-dye binding," *Analytical Biochemistry*, vol. 72, p. 243, 1976.

[41] M. Alhoshan, J. Alam, L. A. Dass, and N. Al-Homaidi, "Fabrication of polysulfone/ZnO membrane: influence of ZnO nanoparticles on membrane characteristics," *Advances in Polymer Technology*, vol. 32, no. 4, Article ID 21369, 2013.

[42] R. A. Damodar, S.-J. You, and H.-H. Chou, "Study the self cleaning, antibacterial and photocatalytic properties of TiO_2 entrapped PVDF membranes," *Journal of Hazardous Materials*, vol. 172, no. 2-3, pp. 1321–1328, 2009.

[43] R. M. Alwan, Q. A. Kadhim, K. M. Sahan et al., "Synthesis of zinc oxide nanoparticles via sol—gel route and their characterization," *Journal of Nanoscience and Nanotechnology*, vol. 5, no. 1, pp. 1–6, 2015.

[44] M. Shoja, K. Shameli, M. B. Ahmad, and K. Kalantari, "Preparation, characterization and antibacterial properties of polycaprolactone/ZnO microcomposites," *Digest Journal of Nanomaterials and Biostructures*, vol. 10, no. 1, pp. 169–178, 2015.

[45] P. Qu, H. Tang, Y. Gao, L.-P. Zhang, and S. Wang, "Polyethersulfone composite membrane blended With cellulose fibrils," *BioResources*, vol. 5, no. 4, pp. 2323–2336, 2010.

[46] G. Wu, S. Gan, L. Cui, and Y. Xu, "Preparation and characterization of PES/TiO_2 composite membranes," *Applied Surface Science*, vol. 254, no. 21, pp. 7080–7086, 2008.

[47] C. Liao, J. Zhao, P. Yu, H. Tong, and Y. Luo, "Synthesis and characterization of SBA-15/poly (vinylidene fluoride) (PVDF) hybrid membrane," *Desalination*, vol. 260, no. 1-3, pp. 147–152, 2010.